Physics Letters B 747 (2015) 299–304

Contents lists available at ScienceDirect

Physics Letters B

www.elsevier.com/locate/physletb

Parity violation in neutron capture on the proton: Determining the weak pion–nucleon coupling

J. de Vries [a,*], N. Li [a], Ulf-G. Meißner [a,b,c,d], A. Nogga [a,b,c], E. Epelbaum [e], N. Kaiser [f]

[a] Institute for Advanced Simulation, Institut für Kernphysik, and Jülich Center for Hadron Physics, Forschungszentrum Jülich, D-52425 Jülich, Germany
[b] JARA – Forces and Matter Experiments, Forschungszentrum Jülich, D-52425 Jülich, Germany
[c] JARA – High Performance Computing, Forschungszentrum Jülich, D-52425 Jülich, Germany
[d] Helmholtz-Institut für Strahlen- und Kernphysik and Bethe Center for Theoretical Physics, Universität Bonn, D-53115 Bonn, Germany
[e] Institut für Theoretische Physik II, Ruhr-Universität Bochum, 44780 Bochum, Germany
[f] Physik Department T39, Technische Universität München, D-85747 Garching, Germany

ARTICLE INFO

Article history:
Received 19 January 2015
Received in revised form 25 May 2015
Accepted 28 May 2015
Available online 3 June 2015
Editor: W. Haxton

ABSTRACT

We investigate the parity-violating analyzing power in neutron capture on the proton at thermal energies in the framework of chiral effective field theory. By combining this analysis with a previous analysis of parity violation in proton–proton scattering, we are able to extract the size of the weak pion–nucleon coupling constant. The uncertainty is significant and dominated by the experimental error which is expected to be reduced soon.

Although parity violation (PV) induced by the weak interaction is well understood at the level of elementary quarks, its manifestation at the hadronic and nuclear level is not that clear. This holds particularly true for the strangeness-conserving part of the weak interaction which induces PV in hadronic and nuclear systems. The Standard Model predicts PV forces between nucleons. However, their forms and strengths are masked by the nonperturbative nature of QCD at low energies. Combined with the difficulty of doing experiments with sufficient accuracy to extract parity-violating signals, hadronic PV is one of the least tested parts of the Standard Model.

The understanding of low-energy strong interactions has increased tremendously by the use of effective field theories (EFTs). It has been realized that by writing down the most general interactions among the low-energy degrees of freedom that are consistent with the symmetries of QCD, one obtains an EFT, chiral perturbation theory (χPT), that is a low-energy equivalent of QCD. Each interaction term in the chiral Lagrangian comes with a coupling strength, or low-energy constant (LEC), which needs to be extracted from data or computed in lattice QCD. In contrast to low-energy QCD itself, χPT allows one to calculate observables in a perturbative framework with expansion parameter p/Λ_χ, where p is the momentum scale of the process and $\Lambda_\chi \sim 1$ GeV, the scale where the EFT breaks down. Although nuclear physics is intrinsically nonperturbative, the nucleon–nucleon (NN) potential can be calculated perturbatively within χPT. The resulting chiral potential is then iterated to all orders to calculate NN-scattering and bound state properties. This framework is usually called chiral nuclear EFT (for recent reviews, see Refs. [1,2]).

The success of chiral EFT in parity-conserving (PC) nuclear physics has led to an analogous program in the PV sector [3–7]. One starts with the four-quark operators that are induced when the heavy weak gauge bosons are integrated out. The next step entails constructing a PV chiral Lagrangian which contains all interaction terms that transform under chiral symmetry in the same way as the underlying four-quark operators. From the resulting chiral Lagrangian one then calculates the PV NN potential and electromagnetic current. In the final step the obtained PV potential and current are applied, in combination with the PC chiral potential and current, in calculations of nuclear processes. The PV LECs appearing in the PV chiral Lagrangian can be fitted to some data and other PV processes can then be predicted.

Although this sounds like a good strategy, in practice this procedure is complicated by the lack of data on PV processes. So far, hadronic PV has only been measured in a handful of experiments (see Refs. [8,9] for recent reviews). The longitudinal analyzing power (LAP), which would be zero in the limit of no PV, has been measured for proton–proton scattering at three different energies [10–12], for proton–alpha scattering only at a single

* Corresponding author.
E-mail address: j.de.vries@fz-juelich.de (J. de Vries).

http://dx.doi.org/10.1016/j.physletb.2015.05.074

energy [13,14], and recently for the first time a preliminary result has been reported for radiative neutron capture on the proton $\vec{n}p \to d\gamma$ at thermal energies [15]. Nonzero parity-violating signals have also been found in more complex systems, as exemplified by the radiative decay of the ^{19}F nucleus [16,17] and the anapole moment of the Cesium atom [18].

The first full chiral EFT analysis of PV nuclear forces has been done in Ref. [3] where it has been concluded that at leading order (LO) only a single interaction term appears:

$$\mathcal{L}_{\not P} = \frac{h_\pi}{\sqrt{2}} \bar{N}(\vec{\pi} \times \vec{\tau})^3 N \ , \tag{1}$$

written in terms of the pion isospin-triplet $\vec{\pi}$, the nucleon isospin-doublet $N = (p, n)^T$, and the weak pion–nucleon coupling constant h_π. The leading order PV potential arising from one-pion exchange takes the form

$$V_{\rm OPE} = -\frac{g_A h_\pi}{2\sqrt{2}F_\pi} i(\vec{\tau}_1 \times \vec{\tau}_2)^3 \frac{(\vec{\sigma}_1 + \vec{\sigma}_2)\cdot \vec{k}}{m_\pi^2 + \vec{k}^{\,2}}, \tag{2}$$

in terms of the momentum transfer $\vec{k} = \vec{p} - \vec{p}\,'$, where $\vec{p}$ and $\vec{p}\,'$ are the incoming and outgoing nucleon momenta in the center-of-mass frame, and $\vec{\sigma}_{1,2}$ and $\vec{\tau}_{1,2}$ the nucleon spin- and isospin-operators, respectively. $F_\pi = 92.4$ MeV denotes the pion decay constant, $m_\pi = 139.57$ MeV the charged pion mass, and $g_A = 1.29$ the nucleon axial-vector coupling constant taking into account the Goldberger–Treiman discrepancy, in order to represent the strong πNN-coupling.

Considering that there are no other terms at leading order, the one-pion exchange (OPE) potential can be expected to give the dominant contribution to PV in nuclear processes. Nevertheless, despite decades of experimental effort the existence of a long-range PV NN force has not been confirmed. This indicates that h_π could be smaller than expected from naive dimensional analysis which predicts $h_\pi \sim G_F F_\pi \Lambda_\chi \sim 10^{-6}$ (consistent with the often-used estimate $h_\pi = 4.6 \cdot 10^{-7}$ of Ref. [19]), with $G_F \simeq 1.67 \cdot 10^{-5}$ GeV^{-2} the Fermi coupling constant. In fact, the isovector nature of the weak pion–nucleon coupling already gives a natural suppression of $\sin^2\theta_w \sim 1/4$ [3,20], while a large-N_c analysis indicates that h_π is even further suppressed [20–22]. A first lattice QCD calculation gave $h_\pi \simeq 10^{-7}$ [23]. Finally, the absence of a PV signal in the γ-ray emission from ^{18}F leads to the bound $h_\pi \leq 1.3 \cdot 10^{-7}$ [24–26].

The evidence in favor of a small value of h_π is not conclusive. Large-N_c arguments can be misleading, especially for pionic interactions, while the lattice calculation did not include disconnected diagrams. The bound from ^{18}F depends on nuclear structure calculations of a relatively complicated nucleus and, despite being a careful work, might suffer from uncontrolled uncertainties. Finally, the Cesium anapole moment prefers a much larger value $h_\pi \simeq 10^{-6}$ although the involved uncertainties are also larger [27,28]. It seems that the only conclusive method of determining the size of h_π is through a fit to experiments using simple few-body processes which are theoretically much better under control. Unfortunately, only a few PV signals have been measured so far in such few-body processes. In recent work we investigated the data on $\vec{p}p$ scattering in a chiral EFT framework [6,29]. The main goal of this paper is to combine this analysis with the recent data on PV in radiative neutron capture on the proton $\vec{n}p \to d\gamma$ and extract a value of h_π. An analysis of PV in the inverse process $\vec{\gamma}d \to np$ within pionless EFT has recently been performed in Ref. [30].

Our task gets complicated by two things. First of all, the OPE potential in Eq. (2) changes the total isospin and does not contribute to $\vec{p}p$ scattering. The three data points still carry information on the size of h_π because the analyzing power does depend on h_π through the two-pion-exchange (TPE) diagrams [5,29,7]. The TPE diagrams appear at higher order in the chiral counting where additional contributions in the form of PV NN contact terms appear as well [5,31,32]. Secondly, although the PV OPE potential does contribute to $\vec{n}p \to d\gamma$ capture, if the coupling constant h_π is really as small as suggested, formally higher-order corrections can become relevant and need to be taken into account. Again such corrections appear as NN contact terms. We discuss these subleading terms in the PV potential and the current at a later stage.

The other ingredients required for the calculation of PV observables are the PC NN potential and the PC and PV electromagnetic currents. As in Ref. [29], we apply here the next-to-next-to-next-to-leading order (N^{3}LO) chiral EFT potential obtained in Ref. [33] and we refer the reader to this paper for all further details. The N^{3}LO potential exists for several values of the cut-off needed to regularize the scattering equation. Here, we regularize the PV potential in the same way as the PC potential via

$$V_{PV}(\vec{p}, \vec{p}\,') \to e^{-p^6/\Lambda^6} V_{PV}(\vec{p}, \vec{p}\,') e^{-p'^6/\Lambda^6} \ , \tag{3}$$

where three choices for $\Lambda = \{450, 550, 600\}$ MeV are applied, see Refs. [29,33]. TPE diagrams are regularized with a spectral cut-off $\Lambda_S = \{500, 600, 700\}$ MeV [33]. In recent work [34] an alternative regularization scheme (formulated in coordinate space) has been proposed which better preserves the long-range nature of pion-exchange terms in the potential. Considering the large experimental uncertainties in the field of nuclear parity violation, we do not expect drastic changes if the alternative regularization scheme is applied. Nevertheless, we will investigate this new scheme and its extension to N^{4}LO [35] in future work.

Within the chiral EFT power-counting rules the dominant PC current arises from the nucleon magnetic moments. At next-to-leading (NLO) order we encounter the one-body convection current,[1] which arises from gauging the nucleon kinetic energy term, and the leading OPE two-body currents. The total PC current up to NLO is then given by

$$\begin{aligned}\vec{J}_{PC} = \sum_{j=1}^{2} \frac{e}{4m_N} \Big\{ -\Big[\mu_s + \mu_v \tau_j^3\Big] i(\vec{\sigma}_j \times \vec{q}) + (1 + \tau_j^3)(\vec{P}_j + \vec{P}\,'_j) \Big\} \\ \times \delta^{(3)}[\vec{P}_j - \vec{P}\,'_j - \vec{q}\,] \\ + \frac{e g_A^2}{4F_\pi^2} i\left(\vec{\tau}_1 \times \vec{\tau}_2\right)^3 \Bigg\{ 2\vec{k} \frac{\vec{\sigma}_1 \cdot (\vec{k} + \vec{q}/2)}{(\vec{k} + \vec{q}/2)^2 + m_\pi^2} \frac{\vec{\sigma}_2 \cdot (\vec{k} - \vec{q}/2)}{(\vec{k} - \vec{q}/2)^2 + m_\pi^2} \\ - \vec{\sigma}_1 \frac{\vec{\sigma}_2 \cdot (\vec{k} - \vec{q}/2)}{(\vec{k} - \vec{q}/2)^2 + m_\pi^2} - \vec{\sigma}_2 \frac{\vec{\sigma}_1 \cdot (\vec{k} + \vec{q}/2)}{(\vec{k} + \vec{q}/2)^2 + m_\pi^2} \Bigg\} \ , \end{aligned} \tag{4}$$

where $\mu_s = 0.88$ and $\mu_v = 4.72$ are the isoscalar and isovector nucleon magnetic moments. The momenta of the incoming and outgoing nucleon interacting with the photon (of outgoing momentum $\vec{q}$) are denoted by $\vec{P}_j$ and $\vec{P}\,'_j$, respectively. The momenta carried by the intermediate pions are $\vec{k} + \vec{q}/2 = \vec{P}_1 - \vec{P}\,'_1$ and $\vec{k} - \vec{q}/2 = \vec{P}\,'_2 - \vec{P}_2$. In contrast, the leading PV current is solely due to OPE diagrams where one of the pion-nucleon vertices is from Eq. (1)

[1] Here the power-counting rules of Ref. [33] are followed where recoil and relativistic corrections are relegated to higher order by counting $1/m_N \sim k/\Lambda_\chi^2$, where k is the typical momentum scale of the process. The magnetic moment operator is not a recoil correction and only scales as $1/m_N$ for conventional reasons. We thus treat $\mu_{s,v}/m_N \sim 1/\Lambda_\chi$ which is also justified by the large value of $\mu_v = 4.72$.

Table 1
Total cross section in mb for unpolarized np capture at $2.52 \cdot 10^{-8}$ MeV lab energy. The first column is the calculated cross section using N^{3}LO chiral potentials and the isovector nucleon magnetic moment μ_v. The second column also includes the leading PC OPE current. The experimental result is from Ref. [36]. Contributions from other currents at this order such as the isoscalar magnetic moment and convection current are negligible.

	Isovector magnetic moment	+PC OPE currents	Experimental result
$\sigma_{\rm tot}$	305 ± 4	319 ± 5	334.2 ± 0.5

Table 2
Contributions to the LAP a_γ in np capture in units of h_π. Part 1 is the contribution from one-body currents only, Part 2 from the isovector magnetic moment in combination with the PC OPE currents and the PV OPE potential, and Part 3 from the interference of the isovector magnetic moment and the PV OPE currents.

	Part 1	Part 2	Part 3	Total
a_γ/h_π	-0.27 ± 0.03	-0.53 ± 0.02	0.72 ± 0.03	-0.11 ± 0.05

$$\vec{J}_{PV} = \frac{e g_A h_\pi}{2\sqrt{2} F_\pi} \left(\vec{\tau}_1 \cdot \vec{\tau}_2 - \tau_1^3 \tau_2^3\right) \times \left\{ 2\vec{k} \frac{\vec{\sigma}_1 \cdot (\vec{k} + \vec{q}/2) + \vec{\sigma}_2 \cdot (\vec{k} - \vec{q}/2)}{[(\vec{k} + \vec{q}/2)^2 + m_\pi^2][(\vec{k} - \vec{q}/2)^2 + m_\pi^2]} - \frac{\vec{\sigma}_1}{(\vec{k} - \vec{q}/2)^2 + m_\pi^2} - \frac{\vec{\sigma}_2}{(\vec{k} + \vec{q}/2)^2 + m_\pi^2} \right\} . \quad (5)$$

These ingredients are sufficient to calculate the LO contribution to the longitudinal analyzing power in $\vec{n}p \to d\gamma$. The details of the actual calculation will be presented in a longer paper [37] and therefore we focus here just on the results.

The longitudinal analyzing power (LAP) in $\vec{n}p \to d\gamma$ capture is defined as

$$A_\gamma(\theta) = \frac{d\sigma_+(\theta) - d\sigma_-(\theta)}{d\sigma_+(\theta) + d\sigma_-(\theta)} = a_\gamma \cos\theta \ , \quad (6)$$

with $d\sigma_\pm(\theta)$ the differential cross section for incoming neutrons with positive/negative helicity and θ the angle between the outgoing photon momentum $\vec{q}$ and the neutron spin. The experiment takes place at thermal energies where the total cross section for np capture is dominated by the nucleon isovector magnetic moment μ_v, while the isoscalar magnetic moment μ_s and the convection current give negligible contributions. At NLO the PC OPE currents add to the cross section at the 5% level as can be seen in Table 1. For comparison, using the AV18 interaction we obtain 324 mbar in good agreement with Refs. [38,39]. The remaining discrepancy of roughly 4% with respect to the experimental result should be removed by higher-order corrections, for example in the form of PC contact and TPE currents. In phenomenological models indeed the remaining discrepancy is explained by heavy-meson-exchange currents [38]. The theoretical uncertainties (1%–2%) quoted in the table are obtained from varying the cut-off parameters in the N^{3}LO potential.

Even in the presence of the PV potential, the numerator in Eq. (6) vanishes if we only include the leading magnetic moment currents. An interference with electric dipole currents, which appear at NLO in the form of the convection and OPE currents, is necessary to obtain a non-vanishing result. The dominant contributions to a_γ then consist of an interference between the isovector magnetic moment and:

1. the one-body convection current in combination with the PV OPE potential,
2. the two-body PC OPE currents in combination with the PV OPE potential,
3. the two-body PV OPE currents.

All these contributions appear at the same order in the chiral counting and we present the results in Table 2. The individual contributions are all of the same order, as expected from the power counting, and suffer only from minor uncertainties due to cut-off variations. However, the total result has a much larger relative uncertainty due to cancellations between the individual contributions. These cancellations were found also in Ref. [40] where the AV18 potential has been applied in combination with the same currents. Our central value is also in good agreement with results based on various phenomenological strong potentials and the Siegert theorem for the electric dipole currents [39,41,42]. These calculations do, however, not provide an uncertainty estimate. In Ref. [43] a smaller uncertainty was found when varying the cut-off (roughly $\pm 0.015\, h_\pi$), but the authors did not vary the strong potential simultaneously. In addition the Siegert theorem was applied for the electric dipole currents. The significant dependence of the total result on the cut-off parameters indicates that the extraction of h_π from data on a_γ is less clean than might be expected.

Having available the prediction for a_γ as a function of h_π, we can now compare to data. For a long time only a bound on a_γ existed

$$a_\gamma = (0.6 \pm 2.1) \cdot 10^{-7}, \qquad a_\gamma = (-1.2 \pm 1.9 \pm 0.2) \cdot 10^{-7}, \quad (7)$$

from Refs. [44] and [45], respectively. Applying our most conservative estimate we obtain an upper bound $|h_\pi| \leq 4.5 \cdot 10^{-6}$ on the weak pion–nucleon coupling. Recently a first preliminary result for a_γ was reported [15]

$$a_\gamma = (-7.14 \pm 4.4) \cdot 10^{-8} \ . \quad (8)$$

This result is based on a subset of the full data taken and an improved result with an uncertainty at the 10^{-8} level is expected in the near future.

To fit h_π we combine the a_γ analysis with that of the LAP in pp scattering. As mentioned, the pp LAP does not depend on the OPE PV potential in Eq. (2) due to its isospin-changing nature. Nevertheless, the pp LAP still depends on h_π due to the TPE potential which appears at NLO. At the same order the PV potential contains PV NN contact terms, but only one combination with low-energy constant C contributes to pp scattering ($C = -C_0 + C_1 + C_2 - C_3$ in the notation of Ref. [6]). The LECs h_π and C were fitted to the pp data in Refs. [29]. In Ref. [6] the fit was slightly improved by including the dominant piece of the N^{2}LO PV potential which does not depend on additional unknown LECs.

We compare the obtained values of h_π and C from the data on the np and pp LAPs in Fig. 1 using the intermediate cut-off values to regularize the potential. In the left panel, the ellipse denotes the contours of a total $\chi^2 = 2.71$ corresponding to a fit to pp data, whereas the red vertical lines denote a fit to a_γ at the one-sigma level. In the right panel, the ellipses denote contours of a total $\chi^2 = 2, 3, 4$ corresponding to a combined fit to the pp data and a_γ. The dashed lines in both panels are obtained if we use the expected future experimental uncertainty, $\pm 1 \cdot 10^{-8}$, of the measurement of a_γ while using the same central value as in Eq. (8). The dashed contours are only there to illustrate what the accuracy could be with better data but should not be used to extract values of the LECs.

From the right panel of Fig. 1 at the level of a total $\chi^2 = 4$ the LECs h_π and C become

$$h_\pi = (0.80 \pm 0.70) \cdot 10^{-6} \ , \qquad C = (-6.0 \pm 3.0) \cdot 10^{-6} \ . \quad (9)$$

Since a χ^2 analysis with so few data points can be misleading we collect in Table 3 the observables for the pp and np systems

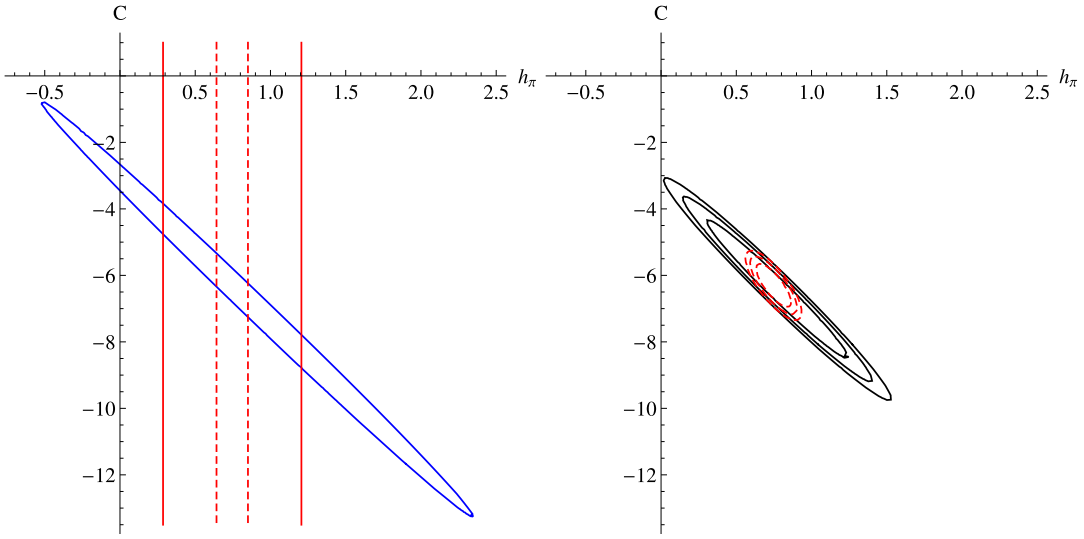

Fig. 1. The allowed ranges for the LECs h_π and C (both in units of 10^{-6}). Left panel: the blue ellipse is a fit to the pp data with a total $\chi^2 = 2.71$ and the vertical solid lines the fit of h_π to a_γ at the one-sigma level. The vertical dashed lines correspond to the same fit, but now using the expected experimental uncertainty ($\pm 1 \cdot 10^{-8}$) keeping the central value as in Eq. (8). Right panel: the black (solid) ellipses are fits to the combined pp and np data with a total $\chi^2 = 2, 3, 4$. The red (dashed) ellipses are the same, but using the expected future experimental uncertainty. (For interpretation of the references to color in this figure legend, the reader is referred to the web version of this article.)

Table 3
Predictions for the pp LAP A_z and a_γ (both in units of 10^{-7}) for three fits using the intermediate cut-off combination. The first fit corresponds to the best-fit value with $h_\pi = 0.77$ and $C = -6.4$. The second and third fits correspond to the values at the edge of the contours with $h_\pi = 0.1$ and $C = -3.0$, and $h_\pi = 1.5$ and $C = -9.0$ respectively (all in units of 10^{-6}). The first three columns correspond to the pp LAP at three different energies and the fourth column to a_γ. The experimental results are from Refs. [10–12,15].

	A_z (13.6 MeV)	A_z (45 MeV)	A_z (221 MeV)	a_γ
Fit 1	-0.90	-1.56	0.57	-0.74
Fit 2	-0.65	-1.36	0.50	-0.10
Fit 3	-0.89	-1.19	0.43	-1.44
Exp.	-0.93 ± 0.21	-1.50 ± 0.22	0.84 ± 0.34	-0.71 ± 0.44

using three different fit values that all lie within the contours of Fig. 1. From Table 3 we see that small (large) values of $h_\pi = 10^{-7}$ ($h_\pi = 1.5 \cdot 10^{-6}$) still give a reasonable fit to the pp data, but underpredict (overpredict) a_γ. However, considering the large experimental uncertainty of a_γ the fits cannot be excluded at a significant level.

To study the dependence of the extraction of the LECs on the details of the strong NN potential, we repeat the analysis for other cut-off values. For $\Lambda = \{450, 550, 600\}$ MeV, respectively, the following best fit parameters emerge

$$h_\pi = \{0.48, 0.77, 1.1\} \cdot 10^{-6} \ ,$$
$$C = -\{4.3, 6.4, 7.4\} \cdot 10^{-6} \ . \qquad (10)$$

We see that the uncertainty in h_π due to cut-off variations is roughly 40%. At present, the experimental uncertainty is still larger. However, once the precision of the a_γ measurement is improved by roughly a factor 2 the cut-off dependence will dominate the uncertainty. The observed cutoff dependence in the predicted value of a_γ is likely to be considerably reduced by the inclusion of higher-order corrections to the exchange currents. One frequently used approach along this line is to make use of the Siegert theorem. We emphasize, however, that such an approach yields only incomplete results for the exchange currents. We postpone a detailed investigation of the role played by higher-order contributions to a future study.

In Fig. 2 we show contours for a total $\chi^2 = 4$ for three different cut-off values. To obtain an allowed range of the LECs, we extract

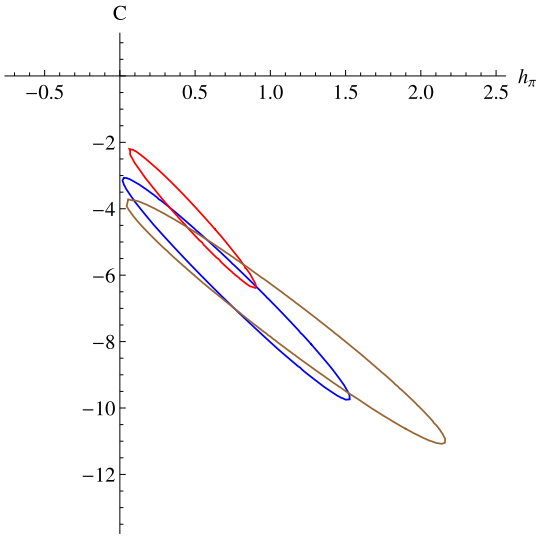

Fig. 2. The allowed ranges for the LECs h_π and C (both in units of 10^{-6}). The ellipses correspond to fits to the combined pp and np data with a total $\chi^2 = 4$ for the three different cut-offs applied (from the smallest to the largest ellipse the cut-off changes from 450 to 600 MeV).

the minimal and maximal values allowed by the three contours. With this conservative approach we obtain the following ranges

$$h_\pi = (1.1 \pm 1.0) \cdot 10^{-6} \ , \qquad C = (-6.5 \pm 4.5) \cdot 10^{-6} \ . \qquad (11)$$

The fits indicate that small values of $h_\pi \sim 10^{-7}$ are barely consistent with the data, with values of $h_\pi \sim (5\text{–}10) \cdot 10^{-7}$ being preferred. Such larger values disagree with the upper limit from ^{18}F gamma-ray emission $h_\pi \leq 1.3 \cdot 10^{-7}$ and lattice and model calculations of $h_\pi \simeq 10^{-7}$. An increase in the accuracy of the a_γ measurement is needed to make a firmer statement about this discrepancy.

So far, our analysis included only the LO contribution to a_γ proportional to h_π. If for whatever reason h_π is small, formally subleading contributions might actually be dominant. The first corrections to a_γ appear two orders down in the chiral expansion and in principle consist of two contributions. The first arises from TPE

diagrams in both the PV potential and currents. However, these contributions are proportional to h_π as well and are then additionally suppressed by the assumed smallness of h_π (in Ref. [43] TPE contributions were found at the 10% level with respect to the OPE result based on the Siegert theorem and a phenomenological *NN* model). The other corrections appear in the form of PV *NN* interactions which contribute both to the PV potential and current. It turns out that the relevant potential and current depend on the same LEC C_4, in the notation of Ref. [6], which is independent of the LEC C appearing in *pp* scattering.

$$V_{\rm PV,NLO} = \frac{C_4}{F_\pi \Lambda_\chi^2} i(\vec{\tau}_1 \times \vec{\tau}_2)^3 (\vec{\sigma}_1 + \vec{\sigma}_2)\cdot \vec{k}, \tag{12}$$

$$\vec{J}_{\rm PV,NLO} = -\frac{C_4}{F_\pi \Lambda_\chi^2}\left(\vec{\tau}_1\cdot\vec{\tau}_2 - \tau_1^3\tau_2^3\right)(\vec{\sigma}_1+\vec{\sigma}_2)\ . \tag{13}$$

Other contact contributions to the PV potential and current appearing at this order give rise to negligible contributions to a_γ.

We obtain the total result for the asymmetry

$$a_\gamma = (-0.11 \pm 0.05) h_\pi + (0.055 \pm 0.025) C_4\ . \tag{14}$$

To estimate the size of the C_4 contributions to a_γ we can use resonance saturation. By comparison with the meson-exchange model of Ref. [19], usually called the DDH model, the LEC C_4 can be expressed as[2]

$$C_4 = \frac{F_\pi \Lambda_\chi^2}{2 m_N}\left[\frac{g_\omega h_\omega^1}{m_\omega^2} + \frac{g_\rho (h_\rho^{1\prime} - h_\rho^1)}{m_\rho^2}\right], \tag{15}$$

in terms of the masses $m_\rho \simeq m_\omega \simeq 780$ MeV and PC couplings $g_\omega = 8.4$ and $g_\rho = 2.8$. We have checked that both the potential and current in Eq. (12) [37] depend on this combination of DDH parameters by comparing to the currents derived in Ref. [27]. The sizes of the PV couplings h_ω^1, h_ρ^1, and $h_\rho^{1\prime}$ are unknown but can be estimated, albeit with significant uncertainty. Taking into account the whole reasonable range for these couplings as obtained in Ref. [19], we find $C_4 = (-0.8 \pm 0.4)\cdot 10^{-7}$. This range includes the more accurate prediction $C_4 = -1.2 \cdot 10^{-7}$ of Refs. [21,22]. To be conservative, we insert the DDH range into Eq. (14) to obtain the estimated uncertainty due to the short-range PV *NN* interaction

$$a_\gamma = (-0.11 \pm 0.05) h_\pi - (0.5 \pm 0.5)\cdot 10^{-8}\ . \tag{16}$$

Considering the current experimental uncertainty of $\pm 4.4 \cdot 10^{-8}$, the contact terms provide only a minor error. This would imply that the above analysis and extraction of h_π is reliable. Small values of h_π are thus disfavored, although formally not (yet) inconsistent. An improvement in the measurement of a_γ will provide a more definite answer regarding the size of h_π. In Refs. [39,42,45] the dependence of the asymmetry on the short-range DDH parameters is found to be smaller than the central value of Eq. (14) by roughly a factor 4 to 5. A possible explanation might be the use of phenomenological strong potentials that typically have a stronger short-range repulsion than the chiral EFT potential, leading to a smaller dependence on short-range operators. A similar effect was found in the study of electric dipole moments [46].

The above reasoning is to some extent circular. We want to fit the LECs from few-body data only, but to estimate the effects of the formally subleading correction we require a model estimate of C_4. This unfortunate situation is due to a lack of data which implies that we cannot fit all LECs at the same time in a consistent way. Some more insight can be obtained by using an alternative strategy. We force h_π to be small and fit the LECs C and C_4 to the *pp* and *np* data. We then obtain the fits in Fig. 3. The blue (solid) contour corresponds to a fit in the C–C_4 plane with a total $\chi^2 = 2.71$ where we set $h_\pi = 0$. In this case the fit prefers values for C_4 which lie outside the range obtained from resonance saturation. The red (dashed) contour corresponds to a fit using $h_\pi = 7.7 \cdot 10^{-7}$ which corresponds to the best fit value for the intermediate cut-off combination. In this case the fit for C_4 is centered around the zero and includes the resonance-saturation range marked by the dotted lines. Although strong conclusion cannot be drawn from this observation, it does indicate that small values of h_π requires short-range contributions that are larger than expected. As always, more and/or more precise data are required to draw firmer conclusions.

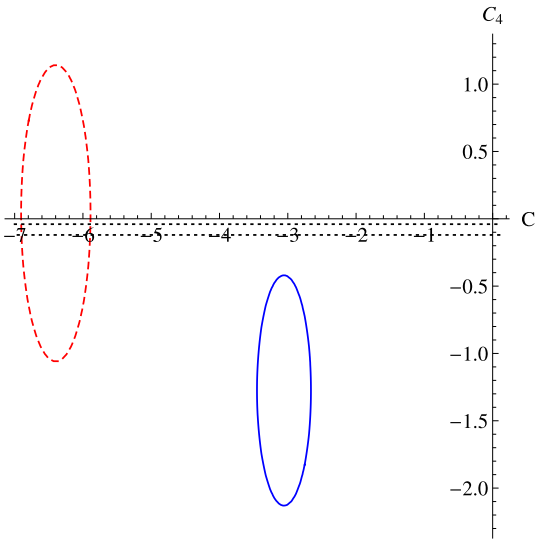

Fig. 3. The allowed ranges for the LECs C and C_4 (both in units of 10^{-6}). The blue (solid) ellipse is a fit to the *pp* and *np* data with a total $\chi^2 = 2.71$ using $h_\pi = 0$. The red (dashed) ellipse is similar but now using $h_\pi = 7.7 \cdot 10^{-7}$ which is the best-fit value for the intermediate cut-off. The dotted horizontal lines mark the predictions made by resonance saturation. (For interpretation of the references to color in this figure legend, the reader is referred to the web version of this article.)

To summarize, in this paper we have extracted the values of two low-energy constants h_π and C appearing in the parity-violating nucleon–nucleon potential and currents. To do so, we have used data on parity violation in proton–proton scattering and radiative neutron capture on a proton target. The extraction has been performed in the framework of chiral effective field theory which has been systematically applied to both the parity-conserving and parity-violating parts of the problem. We have estimated the uncertainties of the fits due to experimental uncertainties, variation of cut-off parameters, and higher-order corrections and find the first of these to be dominant. Our extraction of the weak pion–nucleon coupling constant, $h_\pi = (1.1 \pm 1.0)\cdot 10^{-6}$, is marginally consistent with bounds obtained in experiments on ^{18}F and a lattice QCD calculation. The expected increase in sensitivity of the a_γ measurement will significantly improve the fit and tell whether small values of h_π are consistent with few-body experiments.

Acknowledgements

We thank Christopher Crawford for clarifications regarding the preliminary result of the asymmetry. This work is supported in part by the DFG (CRC 110) and the NSFC (Grant No. 11261130311)

[2] In Ref. [6] the resonance-saturation estimate of C_4 was found to also depend on h_π due to TPE diagrams. However, in the calculation of a_γ we do not include TPE contributions explicitly so these terms should not be subtracted from the estimate.

through funds provided to the Sino-German CRC 110 “Symmetries and the Emergence of Structure in QCD”. We acknowledge the support of the European Community-Research Infrastructure Integrating Activity “Study of Strongly Interacting Matter” (acronym HadronPhysics3, Grant Agreement No. 283286) under the Seventh Framework Programme of EU. Parts of the calculations presented here were performed at the Jülich Supercomputing Center, Jülich, Germany.

References

[1] E. Epelbaum, H.-W. Hammer, U.-G. Meißner, Rev. Mod. Phys. 81 (2009) 1773.
[2] R. Machleidt, D.R. Entem, Phys. Rep. 503 (2011) 1.
[3] D.B. Kaplan, M.J. Savage, Nucl. Phys. A 556 (1993) 653;
D.B. Kaplan, M.J. Savage, Nucl. Phys. A 570 (1994) 833 (Erratum);
D.B. Kaplan, M.J. Savage, Nucl. Phys. A 580 (1994) 679 (Erratum).
[4] D.B. Kaplan, M.J. Savage, R.P. Springer, M.B. Wise, Phys. Lett. B 449 (1999) 1.
[5] S.-L. Zhu, C.M. Maekawa, B.R. Holstein, M.J. Ramsey-Musolf, U. van Kolck, Nucl. Phys. A 748 (2005) 435.
[6] J. de Vries, N. Li, U.-G. Meißner, N. Kaiser, X.-H. Liu, S.-L. Zhu, Eur. Phys. J. A 50 (2014) 108.
[7] M. Viviani, A. Baroni, L. Girlanda, A. Kievsky, L.E. Marcucci, R. Schiavilla, Phys. Rev. C 89 (6) (2014) 064004.
[8] W.C. Haxton, B.R. Holstein, Prog. Part. Nucl. Phys. 71 (2013) 185.
[9] M.R. Schindler, R.P. Springer, Prog. Part. Nucl. Phys. 72 (2013) 1.
[10] S. Kistryn, J. Lang, J. Liechti, T. Maier, R. Muller, F. Nessi-Tedaldi, M. Simonius, J. Smyrski, et al., Phys. Rev. Lett. 58 (1987) 1616.
[11] P.D. Eversheim, W. Schmitt, S.E. Kuhn, F. Hinterberger, P. von Rossen, J. Chlebek, R. Gebel, U. Lahr, et al., Phys. Lett. B 256 (1991) 11.
[12] A.R. Berdoz, et al., TRIUMF E497 Collaboration, Phys. Rev. Lett. 87 (2001) 272301.
[13] R. Henneck, C. Jacquemart, J. Lang, R. Muller, T. Roser, M. Simonius, F. Tedaldi, W. Haeberli, et al., Phys. Rev. Lett. 48 (1982) 725.
[14] J. Lang, T. Maier, R. Muller, F. Nessi-Tedaldi, T. Roser, M. Simonius, J. Sromicki, W. Haeberli, Phys. Rev. Lett. 54 (1985) 170.
[15] Talk given by C. Crawford on behalf of the NPDGamma Collaboration at the 3rd Workshop on the Physics of Fundamental Symmetries and Interactions at Low Energies and the Precision Frontier, PSI, 2013.
[16] K. Elsener, W. Grubler, V. Konig, P.A. Schmelzbach, J. Ulbricht, D. Singy, C. Forstner, W.Z. Zhang, et al., Phys. Rev. Lett. 52 (1984) 1476.
[17] K. Elsener, W. Grubler, V. Konig, P.A. Schmelzbach, J. Ulbricht, B. Vuaridel, D. Singy, C. Forstner, et al., Nucl. Phys. A 461 (1987) 579.
[18] C.S. Wood, S.C. Bennett, D. Cho, B.P. Masterson, J.L. Roberts, C.E. Tanner, C.E. Wieman, Science 275 (1997) 1759.
[19] B. Desplanques, J.F. Donoghue, B.R. Holstein, Ann. Phys. 124 (1980) 449.
[20] D.R. Phillips, D. Samart, C. Schat, Phys. Rev. Lett. 114 (6) (2015) 062301.
[21] N. Kaiser, U.-G. Meißner, Nucl. Phys. A 499 (1989) 699.
[22] U.-G. Meißner, H. Weigel, Phys. Lett. B 447 (1999) 1.
[23] J. Wasem, Phys. Rev. C 85 (2012) 022501.
[24] E.G. Adelberger, M.M. Hindi, C.D. Hoyle, H.E. Swanson, R.D. Von Lintig, W.C. Haxton, Phys. Rev. C 27 (1983) 2833.
[25] S.A. Page, H.C. Evans, G.T. Ewan, S.P. Kwan, J.R. Leslie, J.D. Macarthur, W. Mclatchie, P. Skensved, et al., Phys. Rev. C 35 (1987) 1119.
[26] W.C. Haxton, Phys. Rev. Lett. 46 (1981) 698.
[27] W.C. Haxton, C.P. Liu, M.J. Ramsey-Musolf, Phys. Rev. C 65 (2002) 045502.
[28] W.C. Haxton, C.P. Liu, M.J. Ramsey-Musolf, Phys. Rev. Lett. 86 (2001) 5247.
[29] J. de Vries, U.-G. Meißner, E. Epelbaum, N. Kaiser, Eur. Phys. J. A 49 (2013) 149.
[30] J. Vanasse, M.R. Schindler, Phys. Rev. C 90 (4) (2014) 044001.
[31] L. Girlanda, Phys. Rev. C 77 (2008) 067001.
[32] D.R. Phillips, M.R. Schindler, R.P. Springer, Nucl. Phys. A 822 (2009) 1.
[33] E. Epelbaum, W. Glöckle, U.-G. Meißner, Nucl. Phys. A 747 (2005) 362.
[34] E. Epelbaum, H. Krebs, U.-G. Meißner, Eur. Phys. J. A 51 (5) (2015) 53.
[35] E. Epelbaum, H. Krebs, U.-G. Meißner, arXiv:1412.4623 [nucl-th].
[36] A.E. Cox, S.A.R. Wynchank, C.H. Collie, Nucl. Phys. 74 (1965) 497.
[37] J. de Vries, N. Li, U.-G. Meißner, A. Nogga, E. Epelbaum, N. Kaiser, in preparation.
[38] J. Carlson, R. Schiavilla, Rev. Mod. Phys. 70 (1998) 743.
[39] R. Schiavilla, J. Carlson, M.W. Paris, Phys. Rev. C 67 (2003) 032501.
[40] C.H. Hyun, T.S. Park, D.P. Min, Phys. Lett. B 516 (2001) 321.
[41] C.H. Hyun, S.J. Lee, J. Haidenbauer, S.W. Hong, Eur. Phys. J. A 24 (2005) 129.
[42] C.-P. Liu, Phys. Rev. C 75 (2007) 065501.
[43] C.H. Hyun, S. Ando, B. Desplanques, Phys. Lett. B 651 (2007) 257.
[44] J.F. Cavaignac, B. Vignon, R. Wilson, Phys. Lett. B 67 (1977) 148.
[45] M.T. Gericke, R. Alarcon, S. Balascuta, L. Barron-Palos, C. Blessinger, J.D. Bowman, R.D. Carlini, W. Chen, et al., Phys. Rev. C 83 (2011) 015505.
[46] J. Bsaisou, J. de Vries, C. Hanhart, S. Liebig, U.-G. Meißner, D. Minossi, A. Nogga, A. Wirzba, J. High Energy Phys. 1503 (2015) 104.